Proceedings of the Canadian Society for Mechanical Engineering International Congress
32nd Annual Conference of the Computational Fluid Dynamics Society of Canada
Canadian Society of Rheology Symposium
CSME-CFDSC-CSR 2025
May 25–28, 2025, Montréal, Québec, Canada

Mechanistic Understanding of the Effects of Graphene Oxide on the Thermal Conductivity of Polymer Fuel Cells

Mahsheed Rayhani[1], Cuiying Jian[1*]
[1]Department of Mechanical Engineering, York University, Toronto, Canada
*cuiying.jian@lassonde.yorku.ca

Abstract— Efficient thermal management is critical for the performance and durability of polymer electrolyte membrane fuel cells (PEMFCs), particularly under dry and high-temperature conditions. This study examines the impact of graphene oxide (GO) incorporation on the thermal conductivity (TC) of Nafion membranes using molecular dynamics (MD) simulations. To this end, the TC of 0.8 wt% GO-loaded Nafion membrane was compared with cast Nafion membranes at varying hydration levels. Additionally, the influence of temperature (300 K, 325 K, and 350 K) on TC was evaluated for both cast and GO-loaded membranes. It was found hydration level increment leads to a 14% TC enhancement, which was consistent with the literature results. On the other hand, the addition of GO reduced TC of the dry membrane by 4.7%. For dry membranes, temperature elevation induces slightly negative impacts on TC in both cast and GO-loaded samples. This reduction is primarily attributed to the fragmentation of connected water clusters, which weakens interchain heat transfer pathways. The water clusters' fragmentation is more pronounced with the presence of GO. Further structural and interaction analysis revealed that the strong interactions of GO with water molecules prevented the formation of connected water clusters. These insights provide valuable guidance for optimizing the TC of PEMFC membranes, emphasizing that optimized GO dispersion, hydration control, and functionalization strategies are essential when incorporating GO-based PEMs to ensure efficient heat dissipation and long-term operational reliability.

Keywords-component; PEMFC; Thermal conductivity; GO; Temperature; Dry membrane

I. INTRODUCTION

Recently, the net zero carbon target emission has promoted the adoption of sustainable energy sources like PEMFCs, which offer 60% efficiency [1]. Widely used in transportation, power supply, and military applications [2], PEMFCs rely on polymer electrolyte membranes (PEMs) for performance regulation [3]. Among various PEMs, perfluorosulfonic acid (PFSA) polymers, such as Nafion, are favored for their high ionic conductivity, mechanical strength, and thermal stability [3], [4]. Despite advancements, PEMFCs face challenges like rapid dehydration due to low thermal conductivity, limiting their practical applications [4]. Hence, enhancing thermal stability is crucial for enhancing fuel cell efficiency and durability.

Several experimental studies have been carried out in the literature, focusing on thermal properties of PEMFCs [5], [6]. However, experimental measurement of Nafion membrane's thermal conductivity requires steady-state conditions under long-term operations, which makes it difficult to precisely measure the hydration levels due to the constant water production and evaporation [7]. To shed light on the underlying mechanisms, fundamental studies using MD have drawn significant interests. Chen et al. [7] reported the positive impact of hydration level and negative impact of temperature on TC. Zheng et al. [8] recorded a higher proton mobility and TC for Aciplex with longer side chain length. Contrarily, Fan et al. [9] observed higher TC for polymers with shorter side chains due to improved water cluster connectivity. The impact of water content and temperature on Nafion TC was also examined by Xian et al. [4]. They reported higher TC values at higher hydration levels due to the increased hydrogen binding bridges, which were diminished with increasing temperatures [4].

To improve the TC of fuel cells, the application of graphene-reinforced nanocomposites for advancing the thermal and mechanical properties of different materials is frequently reported [10-12].

This work will look at the effects of graphene-oxide (GO) nanocomposites on the TC of dry Nafion membranes at different temperatures. Interestingly, it was found that GO nanocomposites negatively affect TC under dry and high-temperature conditions. The remainder of this paper is organized as follows: Section II explains the simulation methodology, and Section III discusses the results obtained, followed by final conclusions in Section IV.

The authors are grateful to Lassonde School of Engineering and Natural Science and Engineering Research Council (NSERC) of Canada for their financial support.

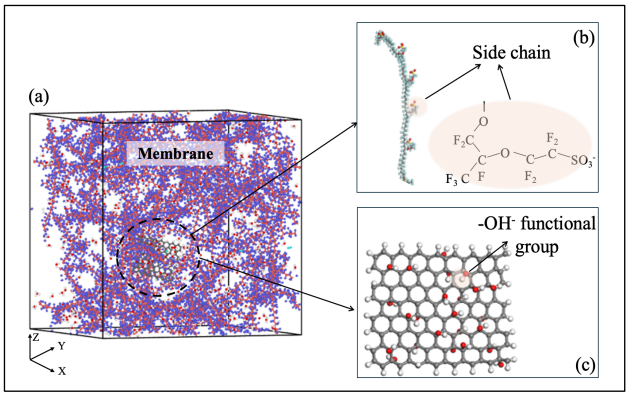

Figure 1. Initial configurations of (a) Nafion membrane at λ=3 with 0.8 wt% graphene oxide (GO). (b) a single chain of Nafion polymer with side chain (c) GO sheet with hydroxyl (OH^-) functional group.

II. METHODOLOGY

A. Simulation details

The initial configuration of all components, including Nafion117 (i.e. 10 repeat units), water, hydronium, oxygen and GO is generated with MedeA® 3.9 software (Materials Design Inc.). To construct the membrane section, 20 Nafion polymers with 200 hydronium ions to neutralize the system. Then, water molecules were simultaneously put inside the simulation box, as depicted in Figure 1. The number of water molecules was determined based on the hydration level, which was calculated according to (1).

$$\lambda = \frac{N_{H_2O}+N_{H_3O^+}}{N_{SO_3^-}}. \quad (1)$$

Here, N_{H_2O} and $N_{H_3O^+}$, and $N_{SO_3^-}$ are the number of water molecules, hydronium ions, and sulfonic acid side chains respectively [4]. In this work, λ was changed from 3 to 9, where λ=3 is denoted as the dry sample with the smallest stable proton form [4]. The samples that include GO were denoted as λ =3_0.8GO (see Table 1). Condensed-phase Optimized Molecular Potentials for Atomistic Simulation Studies (COMPASS) [12] force field was used for partial charges, and the Polymer Consistent Force Field (PCFF) [13] was utilized for intermolecular interactions [14].

In this study, all MD simulations were conducted using Large-scale Atomic/Molecular Massively Parallel Simulator (LAMMPS) [15]. The cut-off distance for the Lennard-Jones parameters is 15×10^{-10} m (15 Å) [14], and Particle-Particle-Particle-Mesh (PPPM) method was employed for long range interactions. The Nose -Hoover thermostats and barostats were used for controlling the temperature. After the annealing processes between 300 K to 600 K, the system was equilibrated under the NPT ensemble for 1 ns to reach the desired temperature (300 K, 325 K, or 350 K). Then, the production run was performed at the corresponding temperature for 2 ns [9]. To calculate TC, the reverse non-equilibrium molecular dynamics (rNEMD) method was used [16]. Each simulation was repeated at least three times to report the standard deviation results.

Table 1. A summary of investigated systems under various temperature and graphene oxide loaded conditions.

System name	*Water content (λ)*	*GO content (%wt)*	*Examined Temperatures (K)*
λ =3	3	0	300, 325, 350
λ = 6	6	0	300
λ =9	9	0	300
λ=3_0.8GO	3	0.8	300, 325, 350

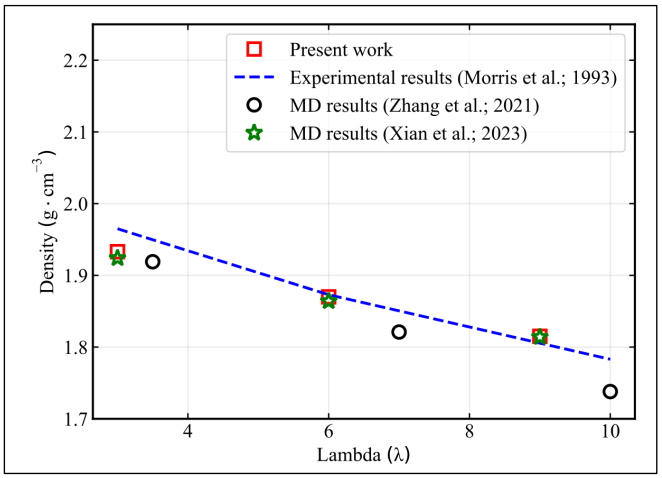

Figure 2. Comparison of density profile for the present work and experimental work of Morris et al. [17], and Molecular Dynamics studies [4], [18] for hydration levels (λ) of 3 to 6.

B. Analyses methods

The analysis of water clusters is reported here to fundamentally understand the effects of hydration levels, temperatures, and GO additions. A water cluster is a collection of water molecules and hydronium ions that remain within a defined cut-off distance [10]. In this work, the cluster size was computed with 3.5 Å cut-off [4] using the Open Visualization Tool (OVITO) software [19]. Furthermore, the cluster connectivity is defined using (2).

$$C_{avg} = \frac{n_{sulfonate}-n_{avg}}{n_{sulfonate}-1}. \quad (2)$$

In (2), $n_{sulfonate}$ is the total number of sulfonic acid groups and n_{avg} is the average number of water clusters. C_{avg} close to zero and 1 indicates poor connectivity, and unified cluster, respectively [9]. Moreover, the Radial Distribution Function (RDF) and Coordination Number (CN) analyses are used to investigate particle-particle interactions. They were calculated using the Visual Molecular Dynamic (VMD 1.9) software [20].

III. RESULTS AND DISCUSSION

In this section, we will first validate the simulation methodology. Then, the TC results will be discussed in detail, along with the relevant analyses.

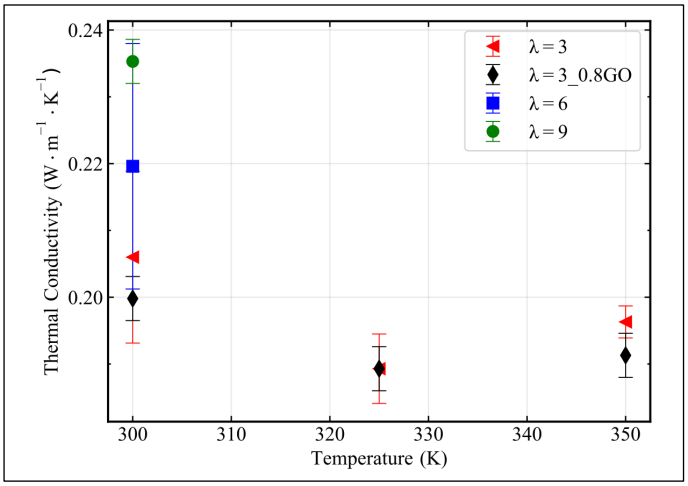

Figure 3. Thermal conductivity results for cast Nafion117 at various hydration levels of 3 to 9, and 0.8 wt% loaded graphene oxide (λ=3_0.8GO) nanocomposite membrane at hydration level of 3 vs temperature.

Table 2. A comparison between thermal conductivity results from current work and the experimental results of Burheim et al. [5].

Water content (λ)	Thermal conductivity (W.m^{-1}.K^{-1})		
	Results of this work	*Experimental results*	*Relative error*
3	0.2060±0.01286	0.1881±0.00980	9.51%
6	0.2196±0.01837	0.1992±0.01160	10.24%
9	0.2353±0.00330	0.2103±0.01340	11.88%

A. Validation

The validation of simulation models was done by comparing the density results of Nafion117 from this study with those of experiments [17] and MD simulations [4], [18]. The results for λ of 3 to 9 are given in Figure 2, which were calculated using the last 0.1 ns of the simulation time. As can be seen, the density results from our study are within 2% error of the literature data, which validated the force fields and method used in this work.

B. Thermal conductivity

TC was first computed with varying λ from 3 to 9. Shown in Table 2, the TC results of Burheim et al. [5] is considered as the reference data, and it can be seen the TC results from our study deviates less than 12% from the experimental results, which is within an acceptable range for MD simulations [4]. The positive impacts of hydration level on TC are also consistent with the MD work of Xian et al. [4]. Therefore, the calculations presented in this research are reliable.

The TC simulation results for all systems are shown in Figure 3. When adding 0.8 wt% GO to the membrane, TC results depict slight reduction from 0.2060±0.01286 W.m^{-1}.K^{-1} (λ=3) to 0.1998 ± 0.00696 W.m^{-1}.K^{-1} (λ=3_0.8GO) at 300 K. With increasing temperature from 300 K to 350 K, a small reduction in TC value was observed for both cases of cast (i.e., 4.70%) and 3_0.8GO sample (i.e., 4.25%). The negative impact of higher temperature on TC of cast Nafion was also reported in the work of Khandelwal et al. [21], where TC was reduced by 18.75% at 338 K compared to that at 300 K [4].

From the above results, increasing the water content significantly enhances TC. Contrarily, the addition of GO to the membrane section exacerbates TC under dry and various temperature conditions. In the next sections, the underlying mechanisms will be discussed.

C. Water cluster size and distribution

It is generally shown that with the increase of water content, larger water clusters are formed due to the enhanced aggregation of water molecules and hydronium ions [18]. The qualitative and quantitative results of cluster distribution with increasing hydration level is represented in Figure 4. For the dry samples (λ=3), cluster distribution depicts scattered and isolated clusters. At higher hydration levels of 6 and 9, the cluster distribution indicates formation of a large and unified cluster. Well-established network of clusters indicates the formation of heat transfer pathways that contribute to better thermal transfer [4].

To probe GO and temperature effects, the total number of clusters and the maximum cluster size are given in Table 3. The average number of clusters were obtained over 2 ns of the simulation. The addition of GO to the membrane results in the formation of smaller, less connected clusters at the same temperature. For instance, in cast Nafion (λ=3) at 325 K, the largest cluster has a size of 1743, but when 0.8 wt% GO is introduced, it shrinks to 1706. In the cast membrane, when increasing temperature, cluster sizes were reduced. Contrarily, nanocomposite samples exhibit an increase in the maximum cluster size from 1488 to 1717 as the temperature rises. However, when considering the average number of clusters, temperature appears to have a minimal impact.

The cluster connectivity results are shown in Figure 5. Notably, connectivity for λ =6 and λ=9 depicts a value closer to 1, which is consistent with the cluster distribution results. However, the presence of GO generally leads to a larger number of isolated clusters across all temperatures, indicating a reduction in cluster connectivity. This reduction directly correlates with a decrease in TC, since a less interconnected network of clusters limits efficient heat transfer [9]. Regarding temperature effects, for the cast sample, cluster connectivity generally decreases, with a significant decline observed at 350 K. Opposite to the cast sample, for the case of nanocomposite membrane, cluster connectivity is not affected by increasing temperatures.

D. Ananlysis of particle-particle interactions

To investigate the particle-particle interactions between water molecules and different particles, RDF and CN results are discussed in this section. The results of this analysis are given in Figure 6 and Figure 7 represents the RDF results of water-water molecules for dry samples under different temperatures. When adding GO to the dry sample (λ =3_0.8GO) at room temperature, the intensity of water-water interactions drops from around 22 to 14. For the case of cast Nafion (λ =3), temperature increase induces a drop in RDF from 21 at 300 K to around 18 at 350 K. In contrast, the RDF of λ=3_0.8GO increased from about 14 to 20 at T=325 K and 18 at T=350 K, suggesting water-water interaction intensifies for the nanocomposite sample upon exposure to the higher temperature.

Water_sulfuric interactions are illustrated in Figure 7 (a). The left-side axis shows the RDF results, while the right-side axis corresponds to the CN results. The CN results for λ=3 shows that more than 2.5 water molecules are around the sulfuric acid groups of Nafion at 300 K, which is reduced to slightly below 2 by increasing temperature. However, for λ=3_0.8GO, the temperature insignificantly affects the number of water molecules surrounding the sulfuric groups. Comparison of the cast and GO-loaded samples under room temperature depicts that when using GO, the number of water molecules around sulfuric acid groups reduces. However, for the GO-loaded samples, increase in temperature seems not to induce any significant changes in the number of water molecules around the sulfuric group.

To assess the interactions between water molecules and GO functional groups, the RDF and CN results for water and hydroxyl groups (OH^-) are given in Figure 7 (b). The graph indicates a persistent interaction between these two components. At all temperatures, these interactions result in approximately 0.1 number of water molecules (i.e. average of 0 to 3 numbers over 2 ns timespan), being localized around the GO functional groups in the first hydration shell. This suggests that water molecules engaged at the GO surface are restricted from participating in the formation of interconnected water clusters, leading to a more scattered distribution of water molecules within the membrane.

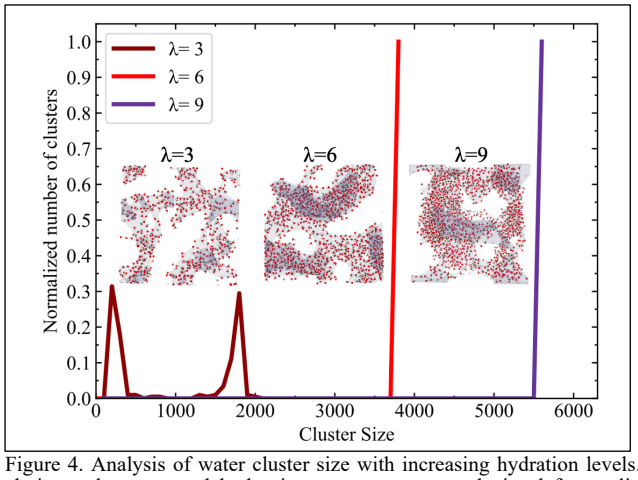

Figure 4. Analysis of water cluster size with increasing hydration levels. For clarity, only water and hydronium components are depicted for qualitative results. Herein, the hydrogen atoms are depicted in white and oxygen atoms are in red.

Table 3. Cluster size and number for cast and nanocomposite dry membranes at different temperatures.

Water content (λ)	*GO content (wt%)*	*Temperature (K)*	*Maximum cluster size*	*Average Number of total clusters*
3	0	300	1912	10.38±2.168
3	0	325	1743	10.43±2.442
3	0	350	1733	12.64±2.703
3	0.8	300	1488	12.07±2.735
3	0.8	325	1706	11.98±2.849
3	0.8	350	1717	12.21±2.725

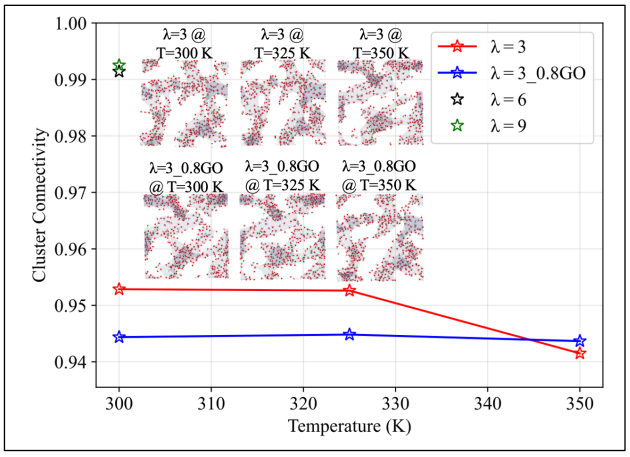

Figure 5. Cluster connectivity results for both cast and nanocomposite membrane samples at different temperatures. The insets are snapshots from our simulations, where the hydrogen atoms are depicted in white and oxygen atoms are in red.

Heat transfer in Nafion membranes primarily occurs through the bridging effect of interchain interactions between sulfonic acid groups (SO_3^-) and water clusters [4]. When adding GO, a part of water molecules approached hydroxyl groups on the GO surface (see Figure 7 and a reduction was observed on the number of water molecules around SO_3^- groups (see Figure 7 (a)). GO competes with SO_3^- groups for hydrogen bonding sites (see Figure 7 (b)), trapping water molecules at its surface. Figure 8 shows schematics for these underlying mechanisms. As was observed in Figure 5 and Figure 7 (a) and (b), the introduction of GO disrupts the natural formation of interconnected water networks (see a comparison in Figure 8), by reducing water-water and water- SO_3^- interactions. This disruption leads to the fragmentation of water clusters, diminishing their connectivity. Consequently, under dry and high-temperature conditions, the presence of GO results in less efficient heat conduction pathways. These findings suggest that the incorporation of GO into membranes for dry, high-temperature PEMFCs may be detrimental, by reducing TC and compromising its overall performance.

This study highlights the need for a strategic approach in integrating GO into PEM membranes, particularly under dry and high-temperature conditions. While GO enhances mechanical stability [11], its effect on TC depends on hydration and temperature levels. Increasing hydration (λ=3 to λ=9) improves TC by 14% due to enhanced heat transfer pathways, whereas GO incorporation in dry membranes (λ=3) reduces TC by 4.7% by trapping water molecules and fragmenting clusters, weakening interchain heat transfer. Temperature further disrupts water cluster connectivity and water-sulfonic acid interactions, though GO-loaded membranes maintain more stable water-sulfur interactions. From a practical standpoint, these findings emphasize the need for optimized GO dispersion, hydration control, and functionalization strategies to mitigate TC drawbacks with GO. Such optimizations are critical for long-

term PEMFC performance in automotive, portable, and stationary fuel cell systems under variable humidity and temperature conditions, providing a foundation for future advancements in high-performance PEMFCs.

IV. Concluding Marks

This study investigates the TC behavior of 0.8 wt% GO-loaded PEMs under dry conditions (λ=3) and elevated temperatures (300 K, 325 K, and 350 K). The key findings are summarized as follows:

- Increasing the hydration level from 3 to 9 enhances the TC by up to 14% due to the formation of well-established heat transfer pathways.
- Incorporating GO into the dry membrane reduces TC by 4.7%. The presence of GO diminishes water-water and water-sulfonic acid interactions and weakens interchain heat transfer via trapping water molecules and fragmenting water clusters.
- The temperature impact on TC is attributed to the disruption of water cluster connectivity and less water-sulfur interactions at higher temperatures.
- For the cast Nafion, increasing temperature significantly reduces the number of water molecules approaching the SO_3^-, while in the presence of GO, water-sulfur interactions remain almost unaffected by increasing temperatures.

These findings offer valuable insights for developing high-performance PEMFCs in dry, high-temperature conditions.

Acknowledgment

The authors acknowledge the computing resources from Digital Research Alliance of Canada.

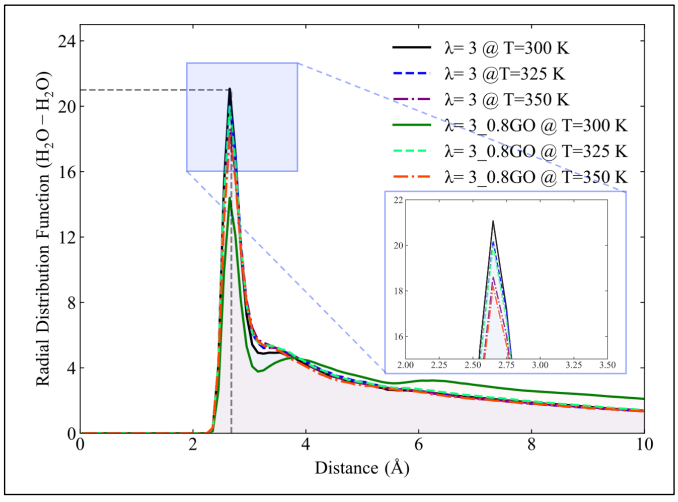

Figure 6. RDF for water-water interactions results of λ=3 samples with and without GO under various temperature conditions.

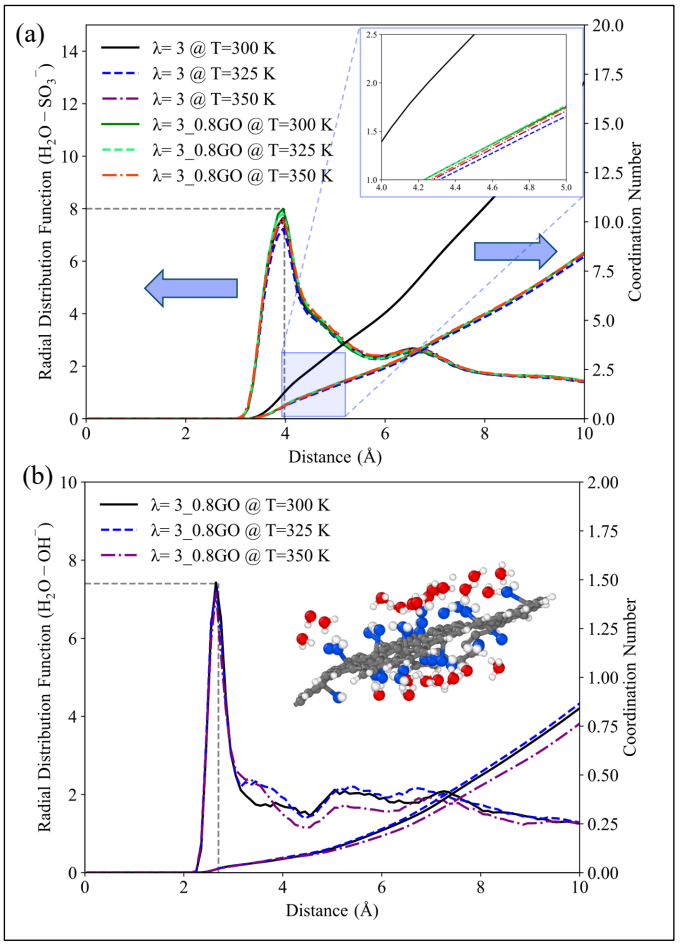

Figure 7. RDF and CN results for λ=3 samples with and without GO under various temperature conditions: (a) RDF and CN for water-sulfuric acid group (SO_3^-). (b) RDF and CN for water-hydroxyl (OH^-) group of GO. Oxygen and hydrogen of OH^- are depicted in blue and white, oxygen and hydrogen for water and hydronium are in red and white, and carbon for graphene is in grey color, respectively.

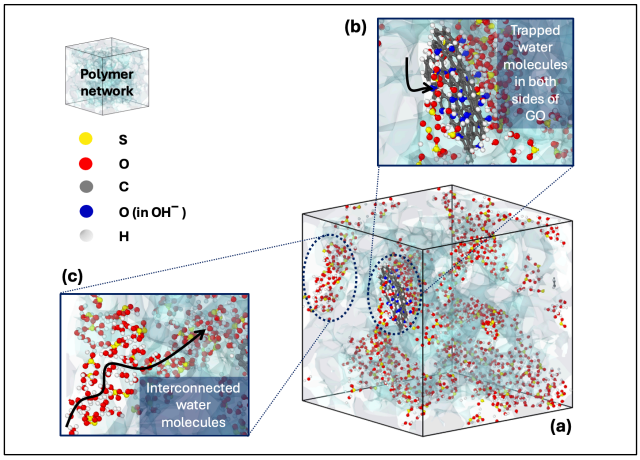

Figure 8. Schematic of trapped water under dry conditions and with GO loaded samples. (a) GO-loaded membranes, (b) trapped water molecules on the GO surface, and (c) interconnected water molecules without GO disruptions.

V. References

[1] U.S. Department of Energy and Energy Efficiency and Renewable Energy, "FUEL CELL TECHNOLOGIES OFFICE."

[2] Battelle Memorial Institute, "Manufacturing Cost Analysis of PEM Fuel Cell Systems for 5- and 10-kW Backup Power Applications."

[3] A. V Lyulin, S. Sengupta, A. Varughese, P. Komarov, and A. Venkatnathan, "Effect of Annealing on Structure and Diffusion in Hydrated Nafion Membranes," *Cite This: ACS Appl. Polym. Mater*, vol. 2020, pp. 5058–5066, 2020, doi: 10.1021/acsapm.0c00875.

[4] L. Xian, Z. Li, S. Li, L. Chen, and W.-Q. Tao, "Elucidating the impact mechanism of temperature and water content on thermal conductivity of hydrated Nafion membranes by molecular dynamics simulation," *Int J Heat Mass Transf*, vol. 208, p. 124034, Jul. 2023, doi: 10.1016/j.ijheatmasstransfer.2023.124034.

[5] O. Burheim, P. J. S. Vie, J. G. Pharoah, and S. Kjelstrup, "Ex situ measurements of through-plane thermal conductivities in a polymer electrolyte fuel cell," *J Power Sources*, vol. 195, no. 1, pp. 249–256, Jan. 2010, doi: 10.1016/j.jpowsour.2009.06.077.

[6] L. Fan, K. Wu, C. Tongsh, M. Zhu, X. Xie, and K. Jiao, "Mechanism of Water Content on the Electrochemical Surface Area of the Catalyst Layer in the Proton Exchange Membrane Fuel Cell," *J Phys Chem Lett*, vol. 10, no. 20, pp. 6409–6413, Oct. 2019, doi: 10.1021/acs.jpclett.9b02549.

[7] L. Chen, H. Zhang, Z.-Z. Li, Y.-L. He, and W.-Q. Tao, "Experimental and Numerical Study on Thermal Conductivity of Proton Exchange Membrane," *J Nanosci Nanotechnol*, vol. 15, no. 4, pp. 3087–3091, Apr. 2015, doi: 10.1166/jnn.2015.9633.

[8] C. Zheng, F. Geng, and Z. Rao, "Proton mobility and thermal conductivities of fuel cell polymer membranes: Molecular dynamics simulation," *Comput Mater Sci*, vol. 132, pp. 55–61, May 2017, doi: 10.1016/j.commatsci.2017.02.022.

[9] L. Fan, F. Xi, X. Wang, J. Xuan, and K. Jiao, "Effects of Side Chain Length on the Structure, Oxygen Transport and Thermal Conductivity for Perfluorosulfonic Acid Membrane: Molecular Dynamics Simulation," *J Electrochem Soc*, vol. 166, no. 8, pp. F511–F518, May 2019, doi: 10.1149/2.0791908jes.

[10] R. Asmatulu, A. Khan, V. K. Adigoppula, G. Hwang, and C. Ramazan Asmatulu, "Enhanced transport properties of graphene-based, thin Nafion® membrane for polymer electrolyte membrane fuel cells," 2017, doi: 10.1002/er.3834.

[11] T. K. Maiti *et al.*, "Molecular dynamics simulations and experimental studies of the perfluorosulfonic acid-based composite membranes containing sulfonated graphene oxide for fuel cell applications," *Eur Polym J*, vol. 174, p. 111345, Jul. 2022, doi: 10.1016/j.eurpolymj.2022.111345.

[12] H. Sun, "COMPASS: An ab Initio Force-Field Optimized for Condensed-Phase ApplicationssOverview with Details on Alkane and Benzene Compounds," 1998. [Online]. Available: https://pubs.acs.org/sharingguidelines

[13] H. Sun, S. J. Mumby, J. R. Maple, and A. T. Hagler, "An ab Initio CFF93 All-Atom Force Field for Polycarbonates," 1994. [Online]. Available: https://pubs.acs.org/sharingguidelines

[14] S. Sengupta and A. V. Lyulin, "Molecular Dynamics Simulations of Substrate Hydrophilicity and Confinement Effects in Capped Nafion Films," *J Phys Chem B*, vol. 122, no. 22, pp. 6107–6119, Jun. 2018, doi: 10.1021/acs.jpcb.8b03257.

[15] A. P. Thompson *et al.*, "LAMMPS - a flexible simulation tool for particle-based materials modeling at the atomic, meso, and continuum scales," *Comput Phys Commun*, vol. 271, p. 108171, Feb. 2022, doi: 10.1016/j.cpc.2021.108171.

[16] F. Müller-Plathe, "A simple nonequilibrium molecular dynamics method for calculating the thermal conductivity," *J Chem Phys*, vol. 106, no. 14, pp. 6082–6085, Apr. 1997, doi: 10.1063/1.473271.

[17] D. R. Morris and X. Sun, "Water-sorption and transport properties of Nafion 117 H," *J Appl Polym Sci*, vol. 50, no. 8, pp. 1445–1452, Nov. 1993, doi: 10.1002/app.1993.070500816.

[18] G. Zhang *et al.*, "Effects of Hydration and Temperature on the Microstructure and Transport Properties of Nafion Polyelectrolyte Membrane: A Molecular Dynamics Simulation," *Membranes (Basel)*, vol. 11, no. 9, p. 695, Sep. 2021, doi: 10.3390/membranes11090695.

[19] A. Stukowski, "Visualization and analysis of atomistic simulation data with OVITO–the Open Visualization Tool," *Model Simul Mat Sci Eng*, vol. 18, no. 1, p. 015012, Jan. 2010, doi: 10.1088/0965-0393/18/1/015012.

[20] W. Humphrey, A. Dalke, and K. Schulten, "VMD: Visual molecular dynamics," *J Mol Graph*, vol. 14, no. 1, pp. 33–38, Feb. 1996, doi: 10.1016/0263-7855(96)00018-5.

[21] M. Khandelwal and M. M. Mench, "Direct measurement of through-plane thermal conductivity and contact resistance in fuel cell materials," *J Power Sources*, vol. 161, no. 2, pp. 1106–1115, Oct. 2006, doi: 10.1016/j.jpowsour.2006.06.092.